Performance of binoculars: Berek's model of target detection

Holger Merlitz[1, *]

[1] *Department of Physics and ITPA, Xiamen University, Xiamen 361005, P.R. China*

compiled: June 20, 2015

A model of target detection thresholds, first presented by Max Berek of Leitz, is fitted into a simple set of closed equations. These are combined with a recently published universal formula for the human eye's pupil size to yield a versatile formalism, capable of predicting binocular performance gains. The model encompasses target size, contrast, environmental luminance, binocular's objective diameter, magnification, angle of view, transmission, stray-light, and the observer's age. We analyze performance parameters of various common binocular models and compare the results with popular approximations to binocular performance, like the well known twilight index. The formalisms presented here are of interest in military target detection, as well as civil applications such as hunting, surveillance, object security, law enforcement or astronomy.

1. Introduction

What can we see through a binocular? Which objects remain hidden, despite of instrumental support offered to our vision? These are fundamental issues, raised with the arrival of the first telescopes and binoculars which supported officers on the battlefields, as well as astronomers under clear skies.

Those among us who are remotely interested in binocular observation know that there exist certain specifications that are related to the performance of such an instrument: A 10x50 binocular has a magnification of $m = 10$ and an objective diameter of $D = 50$ mm. But there also exist additional numbers on the specification sheets issued by the manufacturers, such as the twilight index

$$I_{\rm twilight} = \sqrt{mD}\,, \tag{1}$$

yielding $I_{\rm twilight} \approx 22.4$ for our 10x50 binocular. This number is supposed to tell us something about the twilight performance of the binocular. But what exactly that means remains opaque to most users, and even the trained and experienced sales clerks of specialized optics stores would, at best, cite a deprecated industry norm (DIN 58386), through which the twilight index had once upon a time been defined.

Truth is that this twilight index, just as any other simplified approach to binocular performance, fails to yield numbers that are sufficiently reliable for the evaluation of binoculars in daily life situations. As an example, the popular 8x56 low-light binocular features a twilight index of $I_{\rm twilight} \approx 21.2$, while a 12x42, certainly less common among low-light observers, reaches $I_{\rm twilight} = 22.4$. What is practically unknown beyond the closed circles of human vision experts who evaluate instrumental performance for the purpose of target detection in military applications, is the fact that there exist general purpose models of human vision which can be combined with instrumental optics to deliver quite reliable data about the performance of the combined system, human being plus instrument.

One of these vision models has been presented about 70 years ago by Max Berek, the chief optical designer of Ernst Leitz in Wetzlar, who signed responsible for the first generation photographic lenses of the Leica camera [1, 2]. He then paved the way to combine his theory of vision with the performance of telescopes and binoculars to create a versatile and very general approach to the performance limits for binocular aided observations.

With this article, we want to pay homage to Berek's outstanding achievement, not only because it is of great value to the community of binocular users, but also because the relevance of his approach had subsequently been understated, its accuracy even questioned, by the powerful competition of Carl Zeiss [3]. Since Berek passed away in the same year in which his approach was published, his ideas lacked the push that is required to gain sufficient public attention, to become generally accepted and contribute to the pool of common wisdom.

This article begins with a short and concise introduction to luminance levels in daily life situations (Sec. 2). In Sec. 3 we introduce a common approach to define binocular performance, as presented by H. Köhler and R. Leinhos, and derive the famous twilight index. In Sec. 4 the generalized human vision model of Berek is presented. Since the original data were available only in the form of inconvenient tables, using outdated physical units, we first convert them into modern SI units and apply numerical fit procedures to make them available to the data processing on a computer. A comparison with the results of the Blackwell data set is carried out, followed by a derivation of Ricco's law and the Weber-Fechner law as limiting regimes of Berek's approach. In Sec. 5 we apply the formalism to the unaided eye and evaluate detection ranges of various targets. The proce-

* merlitz@posteo.de

Luminance	White sheet of paper...
0.000001	Detection threshold
0.001	Under clear nightsky
0.1	In moonlight
1	Indoor, running TV
10	Street lighting
100	Indoor lighting
1000	Outdoors, rainy weather
10000	Bright daylight
100000	In direct sunlight

Table 1. Luminance (in cd/m^2) of a white sheet of paper under different ambient light conditions.

dures are then generalized in Sec. 6 to deliver the gain in threshold contrast during observations with many popular binocular types. Distance-range gains with binoculars are discussed in Sec. 7, and our findings are summarized and evaluated in Sec. 8.

2. Luminance levels in daily life

The physical unit of luminous intensity is named candela (cd). One candela roughly corresponds to the luminous intensity emitted by a candle, per steradian of solid angle (reminding here that the sphere, integrated over all directions, would cover a solid angle of 4π steradian). To describe the brightness of an object, we are using its luminous intensity per square-meter (cd/m^2) which then defines the SI unit of luminance.

We may have a few examples to gain some intuition about luminance levels: We imagine a sheet of white paper, and how bright this paper would appear under different ambient light conditions. Table 2 offers a couple of examples, covering the wide range of brightness that occurs between the deepest night and the brightest sunlight (see also Hood et al. [4]).

Luminances of (non-luminous) objects range under daylight conditions between $10-10^5$ cd/m^2, in twilight roughly between $10^{-2}-10$ cd/m^2, while during the night these luminances usually remain below 10^{-2} cd/m^2.

What is special with a white piece of paper is its reflectivity, named albedo, which is close to unity, which means that practically all light that hits the paper is reflected back. Fresh snow does have an albedo above 0.9, while a forest typically has a far lower albedo near 0.1, which means that only 10% of its incident light is reflected back into the environment. If we now imagine a sheet of paper, attached to a tree inside a forest, then we may regard this paper as a target (of albedo $A_t \approx 1$) that is placed in front of the background (of albedo $A_b \approx 0.1$), conveniently assuming that this background is of roughly homogeneous nature. Both, target and background, are exposed to the same ambient light, and their luminances (L_t and L_b, respectively) are therefore proportional to their albedo. We can thus define the (Weber-) contrast of this target against its background [5],

$$C_w = \frac{L_t - L_b}{L_b} = \frac{A_t - A_b}{A_b} \approx 9 \; . \qquad (2)$$

With this in mind, we may now start discussing the various approaches to binocular performance.

3. Resolution gain after Köhler and Leinhos

Binocular efficiency E is commonly defined as [6]

$$E = \frac{R}{r} \; , \qquad (3)$$

where R stands for the range at which a target is detected with the binocular, and r the corresponding range achievable with the unaided eye. In 1957, Köhler and Leinhos [3] of Carl Zeiss published the approximate formula

$$E \sim m^{1-2x} \left(\frac{D}{d_\mathrm{e}}\right)^{2x} T^x \; , \qquad (4)$$

in which m denotes the magnification of the binocular, D its objective diameter, T its transmission, and d_e the eye-pupil diameter. The exponent x is an empirical parameter that is left variable to address different ambient light conditions, namely $x = 0$ in daylight, $x = 1/4$ in twilight and $x = 1/2$ under low-light conditions. As a consequence, this performance index yields an efficiency of $\sim m$ in daylight and $\sim DT^{1/2}$ in the night. Under twilight conditions, and for a particular observer (i.e. a given eye-pupil diameter), the well known twilight index, Eq. (1), emerges, in which the binocular's transmission is omitted. According to Köhler et al., this index is applicable within a background luminance range of 0.003 $cd/m^2 < L_b < 0.3$ cd/m^2. The general validity of this approximation has frequently been questioned: To return to our previous example, the popular 8x56 low-light binocular reaches $I_\mathrm{twilight} \approx 21.2$, while a 12x42 yields a higher twilight index of $I_\mathrm{twilight} \approx 22.4$.

The confusion arises from the fact that there exist quite different approaches to *binocular efficiency*. The Eq. (4) has been derived from observations of test-charts with Landolt rings, which is a classical resolution test, designed to quantify foveal vision acuity. In real life, target detection under low light is rarely resolution, but rather contrast limited. Wild animals, which are active under twilight conditions, are often well adapted to their environment (camouflaged) and represent targets of particularly low contrast. They remain hidden to the observer's eye, even when their apparent angular sizes by far exceed the resolution limits of high contrast targets.

Human vision models, which allow to determine the contrast thresholds of targets under various conditions, have been presented and evaluated before. We may refer to recent approaches, based on the Blackwell-McCready data sets, which are particularly versatile for military applications since they additionally consider parameters such as stimulus duration time [7, 8].

In what follows we present another approach to target detection, introduced during the 1940s by Max Berek. It is a rather minimalist model, but it contains all important ingredients which, in combination with the optical instrument, allow for a reliable evaluation of the binocular efficiency under realistic observation conditions.

4. Berek's human vision model

We assume a circular target of small angular diameter σ and luminance L_t, placed in front of a uniform background of luminance L_b. A typical setup may consist of a distant wild animal of albedo A_t, to be detected in front of a tree-line of albedo A_b. The (Weber-)contrast of the target against its background is then defined in Eq. (2).

We are searching for the threshold contrast C at which this object turns visible to the unaided eye. Berek introduced the following relationship [1],

$$\sqrt{C} = \frac{1}{\sigma}\sqrt{\frac{\phi(L_\mathrm{a})}{L_\mathrm{a}}} + \sqrt{\frac{b(L_\mathrm{a})}{L_\mathrm{a}}}\,, \qquad (5)$$

where L_a stands for the adapting luminance of the observer's eye (in what follows, L_a is assumed to equal the background luminance). The function $b(L_\mathrm{a})$ is the threshold difference in luminance between target and background that allows target recognition. If the angular size σ of the target is large, Eq. (5) simplifies to

$$C \approx \frac{b(L_\mathrm{a})}{L_\mathrm{a}}\,, \qquad (6)$$

called the Weber-Fechner regime [4], in which the recognition of a target turns independent of its size and merely remains a function of the adapting luminance. The meaning of the function $\phi(L_\mathrm{a})$ becomes clear, once Eq. (5) is applied to small targets, so that it may be approximated as

$$\phi(L_\mathrm{a}) \approx \sigma^2 L_\mathrm{a} C\,, \qquad (7)$$

and this relation is known as Ricco's law [9, 10]. It states that for small targets and at constant adapting luminance, the product of threshold contrast, target area and adapting luminance has to be a constant. $\phi(L_\mathrm{a})$ stands for this constant as a function of the adapting luminance L_a. Note that in this expression the angular size σ of the target has to be given in arcmin.

Berek had fitted his functions b and ϕ to measurements conducted with volunteers, and tabulated them in his publications [1, 2]. Figure 1 displays a conversion of these original data into modern physical units, combined with numerical curves, derived from fit procedures, to enable a convenient use of these functions in computer codes. The interpolations yield

$$\log_{10} b = -1.77 + 0.824\,x\,, \qquad (8)$$

with $x = \log_{10}(L_\mathrm{a})$, and

$$\log_{10} \phi = a_0 + a_1 x + a_2 x^2 + a_3 x^3 + a_4 x^4\,, \qquad (9)$$

with coefficients shown in Tab. 2.

The data on which Berek had based his formalism were compiled from publications of Kühl [11] and from unpublished measurements carried out by Martin at

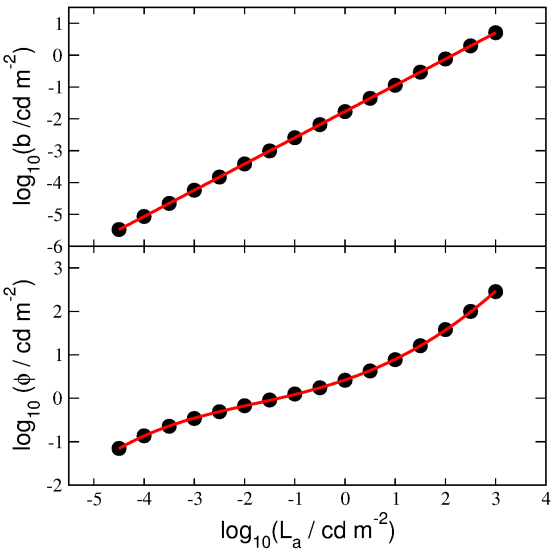

Fig. 1. Numerical interpolations (red curves) of Berek's b-function, Eq. (8), and ϕ-function, Eq. (9). The black dots are Berek's tabulated data.

Emil Busch AG, Rathenow. We shall first compare the predictions of this model with another, more widely available set of measurements, named the Blackwell data set, which was derived independently by Blackwell in 1946 during a laborious series of experiments [12]. The data points in Fig. 2 are taken from Table II of that publication (after conversion into SI-units), solid lines are predictions of Eq. (5). The plot shows that the general trends coincide, although quantitative differences in the threshold contrasts exist. In most situations, the Blackwell data display slightly lower thresholds. Such variations between different visual experiments are not uncommon, because the results do critically depend on details of the laboratory setup (e.g. the amount and distribution of false light that originates from the target and is reflected back from the environment), as well as experience and preparation of the test persons.

There exist numerical parameterizations of the Blackwell data set, and of extended sets by Blackwell-McCready [13], which additionally account for varying stimulation durations. The resulting equations, presented by Matchko et al. [7], are quite complex and contain a plethora of empirically fitted coefficients. Instead, Berek's approach remains comparably simple, and for the purpose of the present paper its accuracy shall

$a_0 = 0.42146$	$a_1 = 0.39557$
$a_2 = 0.07190$	$a_3 = 0.01021$
$a_4 =$ -0.0007959	

Table 2. The coefficients of Eq. (9)

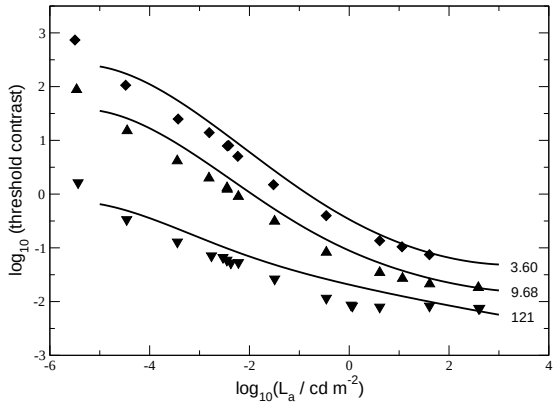

Fig. 2. Threshold contrast as a function of the adapting luminance for different target diameters (values at the right hand side given in arcmin). Solid lines are Berek's parameterization, Eq. (5), symbols are original Blackwell data [12].

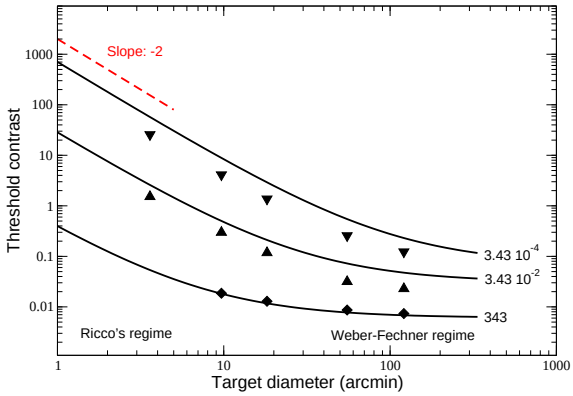

Fig. 3. Threshold contrast as a function of angular target size at three different adaptive luminances (right hand side, in cd/m^2). Curves are from Eq. (5), symbols from the Blackwell data set [12].

be sufficient: First of all, real life situations never feature circular targets or perfectly uniform backgrounds, so that those idealized setups presented here can only offer first approximations to a world of far higher complexity. Apart from that, in what follows we are going to evaluate performance gains, which are ratios of detection thresholds, taken with and without optical instrument, and from such ratios, constant factors (i.e. vertical shifts in Fig. 2) would cancel out. We shall therefore focus on the general thrends that every successful target detection model would have to reproduce:

Figure 3 displays the threshold contrast as a function of the angular target diameter. For small targets, Ricco's law is approximately valid and $C \sim \sigma^{-2}$. With increasing target size, the curves gradually cross over into the Weber-Fechner regime in which C turns invariant of the target size. It is important to note that Ricco's law extends over a wider range of target sizes under low-light conditions, which is a result of extra-foveal receptive fields being active in the retina. Multiple photosensitive rods, covering an increasingly wide area on the retina, converge into single ganglion cells to add up their individual signals [4]. The Blackwell data [12] shown in this figure are taken from Table III of that publication. At daylight, a close agreement is found between Berek's and Blackwell's approach; under low light conditions, Blackwell's data yield somewhat lower detection thresholds. As mentioned above, we shall not regard these differences worrisome: Blackwell's data were gained under ideal conditions inside a well sealed lab and by trained volunteers – the somewhat higher thresholds of Eq. (5) may actually be closer to outdoor situations in which perfectly homogeneous backgrounds are absent.

Note that the albedo 1 of a perfectly white target, when placed into a forest (albedo ≈ 0.1), would yield a Weber contrast of $C_w = 9$. Whenever the threshold contrast in Fig. 3 exceeds that value, self-luminous targets are required to grant visibility.

5. Target detection ranges: Unaided eye

To better understand the features of Eq. (5), we shall now apply the formalism to rather familiar targets that are observed with the unaided eye. We may specify a particular target through its contrast C_w and diameter s (in m), and solve Eq. (5) for the threshold detection range

$$R = s \left\{ 2 \tan \left(\frac{\pi}{180^2} \cdot \frac{\sqrt{\phi(L_\mathrm{a})/L_\mathrm{a}}}{\sqrt{C_w} - \sqrt{b(L_\mathrm{a})/L_\mathrm{a}}} \right) \right\}^{-1} , \tag{10}$$

which denotes the maximum distance at which the target remains visible (note that the numerical factor $\pi/180^2$ arises during the unit conversion of the target half-angle into radian). For simplicity we assume that the observer's eye is adapted to the luminance L_b of a homogeneous background, which may be a forest tree-line. The targets to be observed are located in front of the tree-line, at a considerable distance from the observer. We first compare a wild boar (diameter: 1 m) of low contrast ($C_w = 0.2$) with a white mouse (10 cm) of high contrast ($C_w = 8$). In deep night, the mouse, despite of its small size, is detectable at larger distances than the (well adapted) boar, which only turns visible at distances below 10 m. With increasing light, the curves approach each other and cross, so that under daylight conditions the boar is detectable at distances up to 2 km, now being beyond the mouse's detection distances.

Interesting are self-luminous targets. Let's consider a somewhat idealized candle-flame of diameter ≈ 1 cm. The surface area of the (approximately spherical) flame amounts to π cm^2, and its luminous intensity to one

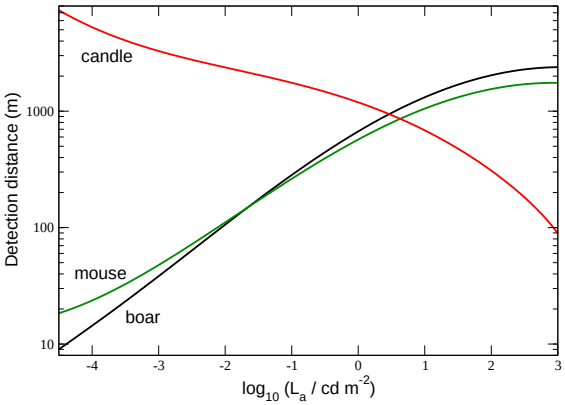

Fig. 4. Detection ranges of a wild boar (diameter: 1 m), a white mouse (10 cm) and a candle (1 cm) at different adapting luminances, obtained from Eq. (10).

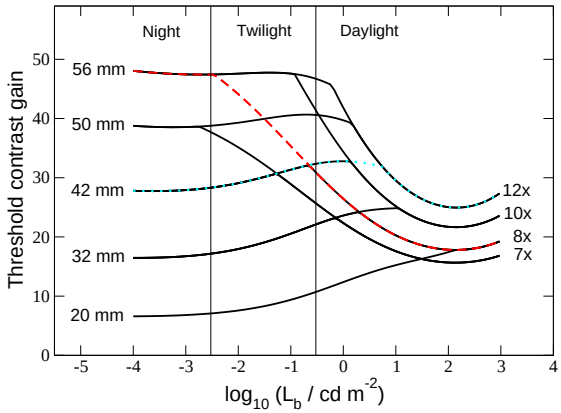

Fig. 5. Binocular performance for an average young observer (below 30 years of age). The 8x56 (dashed line) beats the 12x42 (dotted line) under twilight conditions.

candela. From a distance, we only see a disk of diameter 1 cm, and, for simplicity, assume this disk to feature a homogeneous luminous intensity of $\approx 1/4$ candela. The surface luminosity of that disk is then $\approx \pi^{-1}$ cd cm^{-2} $= 10^4\pi^{-1}$ cd m^{-2}. Note that the candle's brightness does not depend on the environment luminance, so that its contrast to the forest-background (albedo ≈ 0.1) is a function of the background luminance. At night, this contrast is sufficiently high (about $C_w \approx 10^8$) to allow the dark-adapted eye a detection of the candle at distances above 7 km, while in bright daylight the tiny flame turns invisible just a couple of dozen meters away.

This example offers insights that are often misunderstood, but of grave importance for a proper understanding of binocular performance: First, an optical instrument does not necessarily need to resolve a target to grant its visibility; stars, but also distant power lines are well below the resolution threshold, yet, due to their high contrast, easily detectable. On the other hand, even well resolved objects remain invisible as long as they remain below their threshold contrast, and the latter rises rapidly with decreasing daylight. The implications of these insights to the visibility of objects through binoculars are discussed in the following section.

6. Contrast gain with binoculars

We define binocular performance as the inverse of the gain in threshold contrast through the instrument over the unaided eye,

$$E_c = \frac{C}{C_i}\,, \tag{11}$$

where C is the threshold contrast of Eq. (5), and

$$\sqrt{\frac{T}{\mu}C_i} = \frac{1}{\sigma m^*}\sqrt{\frac{\phi(\mu L_\mathrm{b})}{\mu L_\mathrm{b}}} + \sqrt{\frac{b(\mu L_\mathrm{b})}{\mu L_\mathrm{b}}} \tag{12}$$

is the corresponding quantity obtained with the optical instrument [2]. C_i is a straightforward application of Eq. (5) to the virtual image of the binocular. $\mu = T+\lambda$ is the total transmission of the binocular, which is the sum of transmitted "useful" light T and stray-light λ. m^* is the effective magnification of instrument and eye, defined as $m^* = D/d^*$ with the binocular's entrance pupil diameter D and the effective exit pupil diameter d^*. The latter amounts to the smaller of both, the instrumental exit pupil and the eye pupil diameter. We thus obtain

$$E_c = T\left(\frac{\frac{1}{\sigma}\sqrt{\phi(L_\mathrm{b})} + \sqrt{b(L_\mathrm{b})}}{\frac{1}{\sigma m^*}\sqrt{\phi(\mu L_\mathrm{b})} + \sqrt{b(\mu L_\mathrm{b})}}\right)^2\,, \tag{13}$$

which is a positive number and usually larger than unity, since the contrast threshold of the aided eye is lower than the same achievable with the unaided eye.

To determine the effective exit pupil diameter d^*, it is necessary to have a good estimate for the observer's eye-pupil diameter d_e at any level of adaptive luminosity. We employ a universal formula recently presented by Watson et al. [14],

$$d_\mathrm{e} \approx \frac{18.52 + 0.1222f - 0.1056y + 1.386\cdot 10^{-4} fy}{2 + 0.06306f}\,, \tag{14}$$

in which $f = (L_\mathrm{a}a)^{0.41}$ is a function of the adapting luminance and the area of the instrument's subjective field of view, i.e. $a = \pi(\alpha)^2$, α being the maximum half-angle (in degree) of the virtual image. y is the age of the observer (in years), with the restriction of $y \geq 20$. We have rounded all coefficients of Eq. (14) to four significant digits, being sufficiently accurate for our purpose.

With these preparations we are now able to compare the binocular performance as a function of the adaptive luminance L_a. Here we assume a target of small

size (σ = 1 arcmin) in front of a homogeneous background. The unaided eye is once again assumed to be adapted to the background luminance L_b (with a wide subjective half-angle of view of 50°), and the aided eye to the same background luminance, reduced to the transmission of the instrument, μL_b, with an instrumental apparent half-angle of field of 30°. The transmission is assumed to be $\mu = 0.9$, and the usable light $T = \mu$, i.e. we neglect any stray-light contamination.

Figure 5 shows the results of Eq. (13) for a couple of popular binocular sizes. Under bright daylight, the binocular performance is proportional to its magnification (right hand side), and in the night the objective diameter rules the performance (left hand side). Interesting is the crossover behavior under twilight conditions: The vertical lines indicate the luminance range of 0.003 $cd/m^2 < L_b < 0.3$ cd/m^2, for which Köhler et al. determined the validity of their twilight index, Eq. (1). While the latter yields a performance of the 12x42 superior to the 8x56, Fig. 5 clearly demonstrates the superiority of the 8x56 over the entire twilight range, with exception of its upper luminance limit at which the twilight turns into daylight.

The cause of this obvious contradiction is the focus of Köhler et al. on resolution charts, which require high acuity foveal vision to be read out, thus strongly pronouncing the need of magnification, even under conditions in which the latter is boosted at the cost of contrast. Experienced observers would agree that, under twilight conditions, it is not just fine-detail that determines visibility, but a recognition of patterns, contours, directions or movements, and how these visual cues are connecting to individual objects in the context of the background motives. The 8x56 offers a brighter image than the over-magnifying 12x42 [15], and the definition of binocular performance through the threshold contrast seems to reproduce the combined factors that grant recognition of a target more accurately than a purely resolution-based model.

Figure 5 offers a couple of further interesting insights: The compact 8x20 binocular falls dramatically behind in performance once the light turns dim, and well before reaching twilight conditions. Once the observer's eye pupil diameter exceeds the instrument's exit pupil of 2.5 mm, the binocular is used in over-magnification mode and offers a correspondingly dim image. This is a general feature of all curves shown here: Toward lower light, the threshold contrast gain increases, up to the point at which the eye pupil opens beyond the exit pupil of the respective instrument, and then a sharp transition of the performance curve occurs.

Since, with increasing age, the eye pupil diameter of the average observer diminishes, the performance gains of binoculars with large exit pupils diminish as well. Figure 6 shows that the aged observer experiences an 8x56 of significantly reduced contrast gain (red curve). The curve of the 7x50 has disappeared – it is identical with the 7x42, and the latter is outperformed by the 8x42

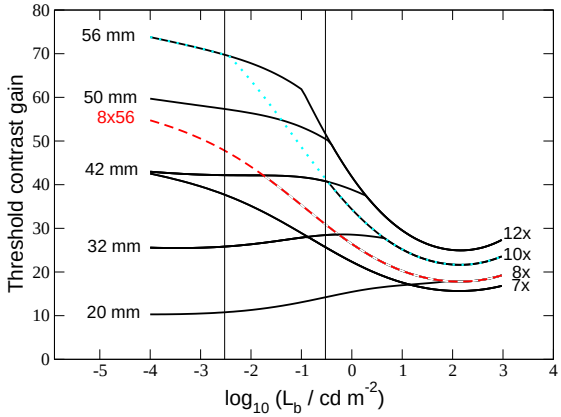

Fig. 6. Binocular performance for an average elder observer (about 60 years of age). The 8x56 (dashed line) performs less favorably, the 10x56 (dotted line) is superior under all conditions.

under all light conditions. A good low-light binocular is the 10x56, the exit pupil of which is still fully usable to the average observer of age between 50-60 years.

7. Detection range gain with binoculars

It is possible to evaluate the threshold detection range of a given object, just as demonstrated in Eq. (10), but now in combination with the binocular, yielding

$$R_i = s \left\{ 2 \tan \left(\frac{\pi}{180^2 m^*} \cdot \frac{\sqrt{\phi(\mu L_\mathrm{a})/L_\mathrm{a}}}{\sqrt{TC_w} - \sqrt{b(\mu L_\mathrm{a})/L_\mathrm{a}}} \right) \right\}^{-1} . \tag{15}$$

We then define the detection range gain as

$$E_r = \frac{R_i}{R} . \tag{16}$$

This quantity is plotted in Fig. 7, for a target of moderate contrast, $C_w = 0.5$, and with binoculars of transmission $\mu = T = 0.9$ (i.e., neglecting any stray-light contamination). Under daylight conditions, the performance gain is almost identical to the magnification of the binocular. This gain in distance then gradually diminishes with the available light, as soon as the eye-pupil diameter exceeds the instrument's exit pupil diameter. As Berek points out, the case

$$\sqrt{TC_w} - \sqrt{b(\mu L_\mathrm{a}/L_\mathrm{a})} \to 0 \tag{17}$$

may in fact arise. This critical point is approached in low light if the target's contrast or the instrument's transmission is sufficiently low. In this case, the detection range gain is not only dropping below unity, but even to zero, implying that through the instrument the target, being still detectable with the bare eye, turns invisible through the binocular. Within this low contrast regime, binocular performance depends critically on its

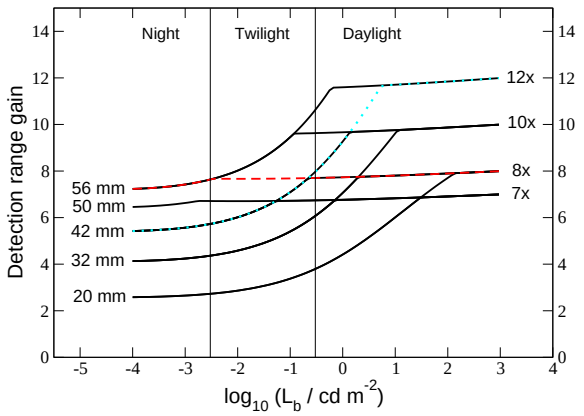

Fig. 7. Detection range gain of various binoculars, evaluated for a young observer (age about 30 years). In twilight, the 8x56 (dashed line) performs higher than the 12x42 (dotted line).

transmission, i.e. in particular on the quality of its anti-reflection coatings.

We note that all computations presented in this section neglect the effects of atmospheric seeing and extinction, which would diminish the visibility of targets at large distances. Assuming a diameter of 0.1 m, the target being considered in Fig. 7 would be detectable to the unaided eye at distances between 4 m (night) and 400 m (daylight), the latter corresponding to observation distances near 5000 m when using a 12x binocular. Here, atmospheric effects would significantly reduce the contrast of the object and yield performance values considerably lower than shown in that graphic. It is possible to account for these seeing effects through the application of a Lambert-Beer type exponential damping of the target contrast,

$$C(r) = C_w \exp(-r\alpha) \; , \tag{18}$$

with a suitable extinction coefficient α, which has the unit of inverse distance.

The parameter α has great potential importance for military target recognition and also for astronomy; however, a detailed discussion of these issues is beyond the scope of this paper. Suffice it to note that under typical "fine weather" viewing conditions, the α-parameter would take values on the order of $\alpha \approx 0.2\ km^{-1}$ in the horizontal viewing direction.

8. Summary

Binocular performance is hard to define consistently, since it requires a careful analysis of the combined system, instrument and observer, and the performance of human vision itself is challenging to model. Berek was among the first who, based on observational data taken with volunteers, developed a general purpose target detection model that incorporated target size, contrast and ambient light conditions. He then applied this model to visual instruments, accounting for the observer's pupil size, instrumental objective size, magnification, transmission and straylight. Using modern approaches to human eye-pupil sizes under any environmental condition, we are now able to add the instrument's apparent angle of view to the equation.

Under twilight conditions, the resulting performance gains differ substantially from a competing approach proposed by Köhler et al. It is important to understand that none of these approaches are wrong; instead, they are focusing on different issues: Köhler and Leinhos measured fine-detail, i.e. foveal acuity, using Landolt rings under various light conditions. Their results are sound and they reflect the resolution gain of the instrument/observer system under these conditions. Yet, target detection, which is simply target sighting, is not solely a matter of resolution, and we have demonstrated how a huge target (wild boar just 10 m away) may remain invisible while a tiny candle flame shines at several km distance due to its tremendous contrast. The contrast thresholds, derived with Berek's theory, often resemble more realistic measures of binocular performance, because target detection under low light is not so much a matter of foveal acuity, but includes elements of extrafoveal pattern recognition, facilitated by information processing through receptive fields inside the human retina.

The evaluations of binocular performance shown in this article were based on a couple of assumptions that are not necessarily satisfied in the field: It was assumed that the binocular was mounted, the target was placed inside its field of view and well focused. When searching for an object of unknown direction and distance, none of these conditions is strictly satisfied. In this case, factors like the objective angle of view, the depth of field and the steadiness of the image during a hand-held panning turn influential. It is therefore safe to claim that each of the performance evaluations has been biased in favor of high-magnification binoculars, because field of view, depth of field and hand-held steadiness are limiting factors that arise particularly at high powers. The field of view is a standard entry of each binocular's specification sheet that deserves no further discussion. Regarding the impact of jitter during hand-held observations, we refer to the analysis offered by Vukobratovich [6] and Yoder et al. [16].

The range of distances E of objects, in which their virtual images appear sharp in the ocular, can be derived as [17]

$$\frac{m^2}{\delta_{akk} + \frac{m^2}{E_{fok}} + \frac{0.001}{d^*}} < E < \frac{m^2}{\frac{m^2}{E_{fok}} - \frac{0.001}{d^*}} \; . \tag{19}$$

Here, δ_{akk} is the accommodation range of the observer (in diopter, being strongly age-dependent), E_{fok} is the distance (in m) onto which the binocular is focused (so that the virtual image of an object of distance E_{fok} is at infinity), m the magnification, and d^* once again

the effective exit pupil diameter (in m). The aperture-related term $0.001/d^*$ arises from the circle of confusion which is tolerated to ascertain the perception of a sharp image. Following König et al. [18], this circle of confusion was chosen to be 3.4 arc-min in the virtual image. When focusing onto the hyperfocal distance, $E(\text{Hyperfokal}) = 1000 \cdot m^2 \cdot d^*$, every object between infinity and the minimum distance

$$E_{\text{m}in} = \frac{m^2}{\delta_{\text{a}kk} + 0.002/d^*} \tag{20}$$

appears in focus. This depth of field diminishes with the square of the magnification, yielding a significant disadvantage of high power binoculars for the detection of targets of unknown distances.

Much is left to be done: Color has been excluded entirely from the vision model. Especially under bright daylight, it is often the color contrast which is of higher relevance to the visibility of fine structures than the brightness contrast. Reliable models of human performance that encompass color vision are still missing, partly because of the high dimensionality of the color space to be explored, and partly due to significant differences in color perception among the observers, which hamper the generalization of individual test results toward versatile multi-purpose performance models.

References

[1] M. Berek, *Zum physiologischen Grundgesetz der Wahrnehmung von Lichtreizen*, Zs. f. Instrumentenkunde **63**, S. 297 (1943).

[2] M. Berek, *Die Nutzleistung binokularer Erdfernrohre*, Z. Phys. **A 125**, S. 657 (1949).

[3] H. Köhler und R. Leinhos, *Untersuchungen zu den Gesetzen des Fernrohrsehens*, Opt. Acta **4**, S. 88 (1957).

[4] D.C. Hood and M.A. Finkelstein, *Sensitivity to Light*, in *Handbook of Perception and Human Performance*, K. Boff, L. Kaufman and J. Thomas (Eds.), New York: Wiley, 1986

[5] Note that the Michelson contrast would be defined as $C_M = \frac{L_t - L_b}{L_t + L_b}$.

[6] D. Vukobratovich, *Binocular performance and design*, Proc. of SPIE **1168**, *Current Developments in Optical Engineering and Commercial Optics*, ed. R.E. Fischer, H.M. Pallicove, W.J. Smith (1989).

[7] R.M. Matchko and G.R. Gerhart, *Parametric analysis of the Blackwell-McCready data*, Optical Engineering 37, p. 1937 (1998).

[8] R.M. Matchko and G.R. Gerhart, *ABCs of Foveal Vision*, Optical Engineering 40, p. 2735 (2001).

[9] E. Baumgardt, *Threshold quantal problems.* In D. Jameson & L. M. Hurvich (Eds.), Handbook of sensory physiology (Vol. 7/4). New York: Springer Verlag, 1972.

[10] Leonard Matin, *Ricco's Law: Response as a power function of stimulus luminance and distance from target center*, Vision Research **15**, p. 1381 (1975).

[11] A. Kühl, Z. Phys. **37**, p. 912 (1936).

[12] H. Richard Blackwell, *Contrast Thresholds of the Human Eye*, J. Opt. Soc. Am. **36**, p. 624 (1946).

[13] H. R. Blackwell and D. W. McCready, *Foveal detection thresholds for various duration of single pulses*, Univ. of Michigan Engineering Research Inst. report #2455-13-F (June 1958).

[14] Andrew B. Watson and John I. Yellott, *A unified formula for light-adapted pupil size*, Journal of Vision **12**, p. 1 (2012).

[15] We are talking about a visual instrument being operated in over-magnification mode, whenever the observer's eye pupil diameter exceeds the exit pupil diameter.

[16] P.R. Yoder, Jr., D. Vukobratovich, *Field Guide to Binoculars and Scopes*, SPIE PRESS Bellingham, Washington USA (2011).

[17] H. Merlitz, *Handfernglaeser; Funktion, Leistung, Auswahl*, Verlag Europa Lehrmittel, Haan-Gruiten (2013), ISBN 978-3-8085-5774-7.

[18] A. König, H. Köhler, *Die Fernrohre und Entfernungsmesser*, Springer-Verlag, p. 123, (1959).